High-sensitivity measurements of $^{12}CH_3D$ pure rotational lines in ground and excited vibrational states in the subTHz region

M.A. Koshelev [a,*], I.N. Vilkov [a], O. Egorov [b,c], A.V. Nikitin [b], M. Rey [d]

[a] Microwave Spectroscopy Laboratory, Institute of Applied Physics RAS, 46 Ul'yanov St, Nizhny Novgorod, 603950, Russia
[b] Laboratory of Theoretical Spectroscopy, V.E. Zuev Institute of Atmospheric Optics SB RAS 1, Akademician Zuev Sq., Tomsk, 634055, Russia
[c] Laboratory of Quantum Mechanics of Molecules and Radiative Processes, Tomsk State University 36, Lenin Ave., Tomsk, 634050, Russia
[d] Groupe de Spectrométrie Moléculaire et Atmosphérique UMR CNRS 7331, UFR Sciences, BP 1039, 51687, Reims Cedex 2, France

ABSTRACT

Pure rotational transitions of $^{12}CH_3D$ having intensity down to 7.9×10^{-30} cm/molecule were studied with a high sensitive spectrometer with radio-acoustic detection of absorption. Among the 14 measured spectral lines, 11 correspond to the rotational transitions within the first three excited states of $^{12}CH_3D$. The theoretical description was carried out using an effective polyad model expressed in irreducible tensor form including a Triad of interacting bands. An accurate set of ground state rotational and centrifugal distortion constants was determined using a simultaneous weighted fit of experimental transitions available in the literature together with the new subTHz measurements. The pressure broadening and shifting parameters of the $J_K = 1_0-0_0$ ground state rotational lines were measured. The shift coefficients of the ground state rotational lines $^Q R(J,K)$ with $J_{max} = 5$ were estimated using the data for the lines of excited vibrational bands and confirmed our experimental results. The information on pressure shifting allowed evaluating possible systematic errors of determining line positions.

1. Introduction

Deuterated chemical compounds are of great interest for astronomical applications. Determination of the D/H ratio by spectral analysis was the subject of numerous works since this permits testing models of Galactic chemical evolution. Highly contrasting D/H ratios in different parts of the Universe have been obtained, which stimulated challenging cosmochemical studies ([1,2] and references therein).

Methane (CH_4) is one of the most abundant gases in planetary atmospheres. CH_4 and its monodeuterated isotopologue CH_3D have been observed on the planets of the solar system and some larger moons, in particular, on Jupiter, Titan, Saturn, Uranus, and Neptune (see [3–7] and references therein). Methane on Mars attracts great interest since it might be a sign of the microbial life or organic matter by analogy with the biological origin of methane in the Earth's atmosphere. Although pure rotational transitions in CH_4 are forbidden by symmetry in the rigid rotor approximation, a very weak absorption can be detected due to centrifugal distortions [8]. The permanent electric dipole moment of CH_3D induced by isotopic substitution is much larger than that rotationally

induced in CH_4 but is still quite small (~0.006 D) [9,10]. Therefore, the investigation of CH_3D spectra in the THz region is a challenging task requiring high spectrometer sensitivity.

The first low resolution spectrum of $^{12}CH_3D$ (hereafter CH_3D) was recorded by Ozier et al. [9] in the 40–120 cm^{-1} (1.2–3.6 THz) frequency range using a grating spectrometer. Ten rotational lines identified as R(5) to R(14) transitions were observed. Despite no K-structure was registered, the values of the dipole moment and the spectroscopic molecular constants were determined. Later, high resolution recordings of the $J_K = 1_0-0_0$ line near 232.6 GHz were obtained by Pickett et al. [11] and by Womack et al. [12], who also measured two lines $J_K = 2_0-1_0$ and $J_K = 2_1-1_1$ around 465.25 GHz for analysis of the telescopic observation toward Orion-KL. Lantanzi et al. [13] reported twelve new rotational transitions in the 697–1162 GHz range corresponding to the next series with 3_K-2_K, 4_K-3_K, and 5_K-4_K. The spectral range was further extended in the work by Drouin et al. [14], where the 7_K-6_K series was recorded. In Ref. [14] the 5_K-4_K series was also re-measured with 100 kHz uncertainty because of small inconsistency with the data of Lattanzi et al. In the recent work by Bray et al. [15,16], the photomixing CW-THz spectrometer provided a relatively broad spectral coverage from 7_K-6_K to 11_K-10_K series. As a result of these studies, line positions are currently known for 70 lines with a relative uncertainty of 10^{-7} and an accurate set of ground state molecular spectroscopic constants was obtained from the global fit analysis [15].

Intensities of 51 transitions were measured in the work [15,16], with the estimated accuracy of 25% providing a set of the dipole moment components. Almost all the lines studied have intensity of about 10^{-25} cm/molecule or higher. However, many weaker lines of hot band transitions located in the range of the rotational spectra can validate the theory completeness and accuracy.

Note that the data sets for the ground state rotational transitions of CH_3D in HITRAN [17], GEISA [18], JPL [19] and Cologne databases [20] are quite different, whereas information concerning CH_3D transitions in this range is not available in TDS [21] or MeCaSDa [22] compilations. To the best of our knowledge, the CH_3D transitions in the subTHz region within excited vibrational states have not been included in the existing databases.

In this work, we present the revised accurate measurements of the ground state transitions (1_0–0_0, 2_0–1_0, and 2_1–1_1) and the first measurements of the pure rotational transitions within ν_6, ν_3, and ν_5 excited states of CH_3D. Lines were recorded in the frequency range up to 0.5 THz using a spectrometer with radio-acoustic detection of absorption (RAD spectrometer) [23–25]. The intensity of the studied lines varied from 10^{-26} to less than 10^{-29} cm/molecule. A new accurate set of rotational parameters of the effective Hamiltonian expressed in irreducible tensors was determined by combining all the transitions measured in the THz region with those calculated by the so-called ground state combination differences (GSCD) method. Pressure broadening and shifting of the 1_0–0_0 ground state rotational line were accurately measured. Shift coefficients of the ground state rotational lines $^QR(J,K)$ with $J_{max} = 5$ estimated using the data on the lines of the excited vibrational bands confirmed our experimental results. The information on pressure shifting allowed estimating possible systematic errors of determining line positions.

2. Experimental details

A spectrometer with radio-acoustic detection of absorption (RAD spectrometer) was used for recording weak CH_3D lines. A detailed description of the spectrometer can be found elsewhere [23–25]. Briefly, the method is based on registering pressure variations induced in a gas due to molecular absorption of radiation modulated by frequency or amplitude. A significant improvement of the spectrometer sensitivity can be achieved by an increase of the radiation power. In this study, the spectrometer was equipped with two types of continuous wave radiation sources. The first one was a series of three backward wave oscillators (BWOs) covering a frequency range of 179–535 GHz, with the output power varying from a few milliwatts to about 50 mW (see [26] and references therein). The second source was a gyrotron operating in a narrow frequency interval of about 1 GHz around 263.5 GHz with a maximum power of 1 kW [27]. Both sources were frequency stabilized by the PLL system against a harmonic of a high stable signal of the microwave synthesizer (Anritsu MG3692C) providing a relative frequency stability of about 10^{-10} and a narrow spectrum bandwidth down to 1 Hz or less [28]. The use of the GPS Time and Frequency System (SR FS740) as a reference oscillator provided frequency setting accuracy and long term stability. The modulation of the radiation frequency by a square-wave signal followed by demodulation at a synchronous detector was used for reducing the baseline effect when recording weak lines. For this purpose, an arbitrary waveform generator (Tektronix AFG3101 and Rohde & Schwarz HFM2550), which permits modulating the radiation frequency with a preset modulation index, was employed in the PLL as a source of a reference signal for the phase detector. Synchronous detection of the absorption signal was done both at the fundamental (for BWO) and the second (for gyrotron) harmonics of the modulation frequency.

A single-pass cell with 10-cm length and 2-cm diameter connected to a microphone was used. The cell was equipped with 2-mm thick conical HDPE windows. All spectra were recorded at room temperature 297 ± 1 K. For the line frequency measurements, the pressure of CH_3D in the cell was about 0.4–0.5 Torr, which seems to be an optimal compromise from the point of view of the RAD spectrometer sensitivity, line width and baseline influence on line shape. Gas pressure was measured using the MKS
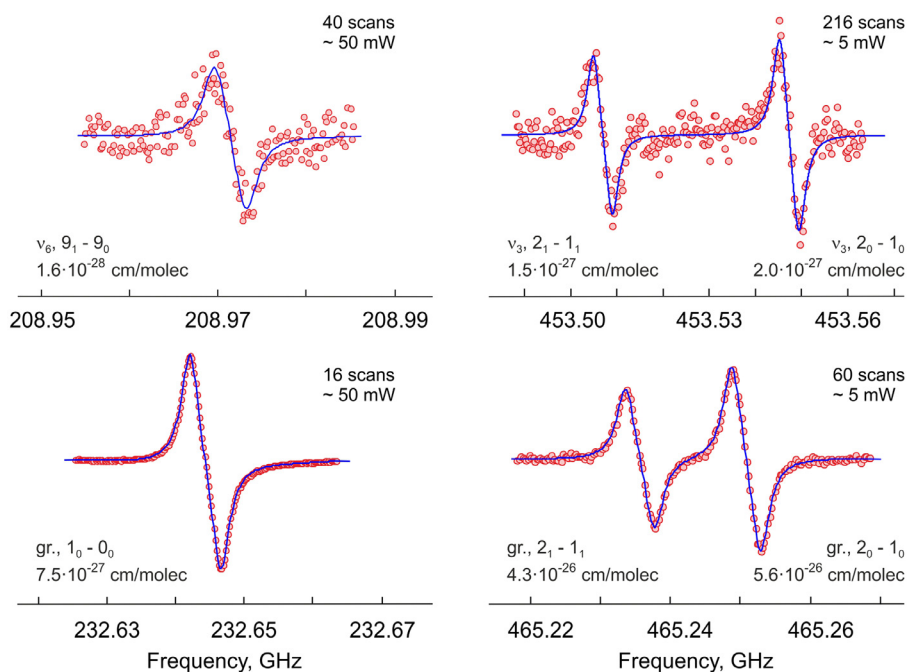

Fig. 1. Averaged experimental spectra of CH_3D obtained using RAD spectrometer with BWO are shown by red circles. The number of averaged scans (time constant 0.5 s/point) and approximate radiation power are given near each spectrum together with line parameters (assignment and intensity). Solid lines are fitted model functions.
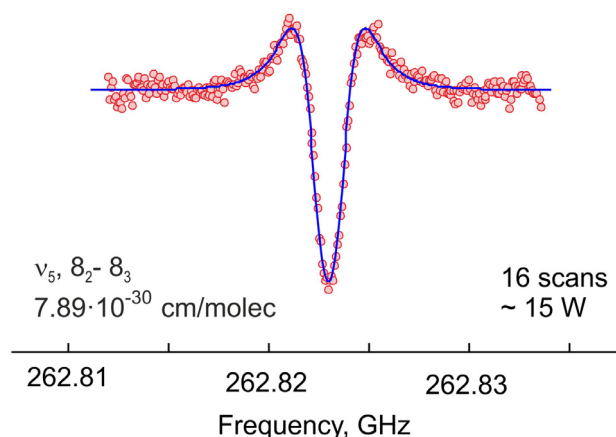
Fig. 2. Averaged experimental spectra obtained at 0.3 Torr of CH_3D using RAD spectrometer with gyrotron are shown by red circles. The total of 78 scans obtained with lock-in time constant of 0.1 s/point were averaged, which is equivalent to averaging of 16 scans with 0.5 s/point (for comparison with Fig. 1). Line parameters and acquisition details are presented in the insets. Solid line is a fitted model function.

Baratron (Type 626B) gauge having a declared accuracy of 0.25% of reading. Commercial methane gas enriched with at least 90% of the $^{12}CH_3D$ isotopologue was used in the study.

High stability of the experimental conditions (parameters of laboratory air, radiation and gas sample) allowed averaging a large number (up to 216) of repeated single scans without noticeable distortions in the observed spectra. The obtained signal-to-noise ratio (SNR) of 10 or higher was sufficient for accurate determination of the central frequencies of the weak CH_3D lines. The acquisition parameters of a single scan were the following: 200–300 frequency points, lock-in time constant 0.5 s for experiments with BWO and 0.1 s for gyrotron. The accumulation time was up to 7.5 h. Examples of the experimental spectra of CH_3D obtained using the RAD spectrometer are shown in Fig. 1 for the BWO and in Fig. 2 for the gyrotron.

3. Spectra analysis and lineshape parameters

A model function based on the Voigt profile was fitted to the experimental spectra and the line shape parameters were determined. The measured central frequencies are presented in Table 1 along with the experimental details (number of averaged recordings and SNR) and spectroscopic information (calculated intensities and assignment) on the studied lines.

The self-broadening and self-shifting parameters of the rotational spectrum lines of CH_3D were estimated on an example of our "best quality" (in terms of SNR) ground state line $J_K = 1_0–0_0$ near 232.644 GHz. This line was studied at six pressures in the 0.26–1.04 Torr range. For each spectrum the modulation depth was preset to be approximately equal to the line half width at half maximum (HWHM) and this value was fixed in the model function. Both multispectra (Fig. 3) and single-spectra fitting procedures were applied and demonstrated the same results for the line shape parameters. SNR for the line recordings was 110–440. The pressure dependence of the line width and center position obtained from the single-spectra fitting is shown in Fig. 4.

The self-broadening and shifting parameters determined by both fitting procedures are 3.285(30) MHz/Torr and 0.085(25) MHz/Torr, respectively. The errors are threefold uncertainties obtained from the spectra fitting, which seems to be a reasonable estimate taking into account possible sources of inaccuracies (finite SNR, pressure and temperature measurement, gas impurities and others). Our measured self-broadening coefficient is about 4.5% less than the value tabulated in HITRAN [17] with 2–5% uncertainty based on IR measurements [29]. The only previous measurement of the self-broadening of the THz lines of CH_3D was done by Bray et al. [15] for the $^QR(7)$ multiplet. The experimental values obtained with total uncertainty of 25% for six K-structure lines are scattered in the 0.079–0.09 cm^{-1}/atm (3.11–3.55 MHz/Torr) interval and no K-dependence was observed. Our accurate value of self-broadening coefficient confirms the results of Bray et al. [15] demonstrating as well a good general agreement with the IR measurements in several excited vibrational bands (see, e.g., Fig. 5 in [15] and references therein).

Table 1

Measured pure rotational transition of CH_3D in the ground and excited vibrational states. The errors are 1-σ fitting uncertainty. The intensities are presented for 100% of $^{12}CH_3D$.

Frequency in MHz	Δ [d]	Intensity in 10^{-28} cm/molecule	Number of averages	SNR[e]	Assignment [f]	
					$v' – v''$	J' K' Γ' – J'' K'' Γ''
196,367.890(240)	265	0.715	50	12	1 – 1	11 1 E – 11 0 E
208,971.359(85)	−83	1.640	40	10	1 – 1	9 1 E – 9 0 E
219,282.532(48)	−14	2.978	40	13	1 – 1	7 1 E – 7 0 E
225,694.315(52)	72	4.035	30	16	1 – 1	5 1 E – 5 0 E
226,757.394(42)	120	2.725	50	22	2 – 2	1 0 A – 0 0 A
227,493.903(57)	33	4.133	36	15	1 – 1	4 1 E – 4 0 E
228,590.864(46)	−67	3.823	50	17	1 – 1	3 1 E – 3 0 E
229,493.023(67)	29	2.018	100	14	1 – 1	1 1 E – 1 0 E
232,644.261(10) [a]	−32	75.19	16	400	0 – 0	1 0 A – 0 0 A
232,644.301(75) [b]	9					
232,644.327(18) [c]	33					
262,822.959(20)	−1	0.0789	16	35	3 – 3	8 2 E – 8 3 E
453,506.92(11)	−65	15.36	216	16	2 – 2	2 1 E – 1 1 E
453,547.12(10)	−94	20.51	216	19	2 – 2	2 0 A – 1 0 A
465,235.540(75) [b]	−29	429.0	60	70	0 – 0	2 1 E – 1 1 E
465,235.553(13)	−17					
465,250.691(75) [b]	−25	560.0	60	95	0 – 0	2 0 A – 1 0 A
465,250.725(10)	8					

[a] pressure shifting was taken into account.
[b] results of Womack et al. [12].
[c] result of Pickett et al. [11].
[d] difference between the observed and calculated wavenumbers in kHz.
[e] SNR was determined as a ratio of peak-to-peak signal amplitude to the noise standard deviation.
[f] $v = 0, 1, 2$ and 3 correspond to $000000(A_1)$, $000001(E)$, $001000(A_1)$, and $000010(E)$ vibrational states A means absence of information on A_1–A_2 splitting.
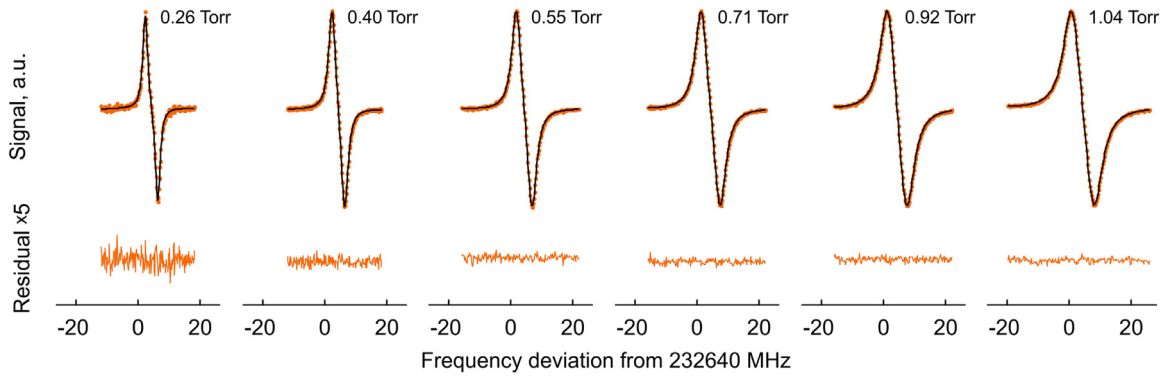
Fig. 3. Experimental line recordings of the ground state rotational transition $J_K = 1_0-0_0$ obtained at different pressures and the result of multispectra fitting. Pressure values are presented for each recording. Magnified (x5) residuals are demonstrated in the lower part.
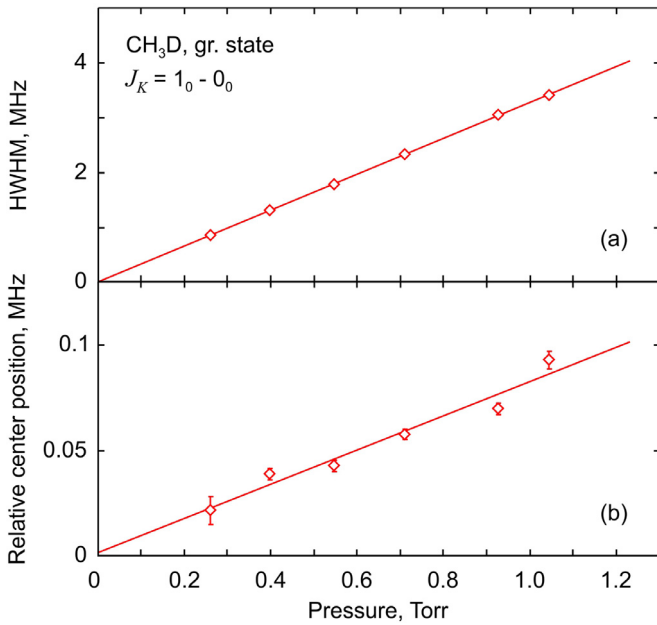

Fig. 4. Pressure dependence of line shape parameters of the ground state rotational transition $J_K = 1_0-0_0$: (a) HWHM and (b) relative center position shifted by 232,644.26 MHz. Error bars are statistical uncertainties obtained from spectra fitting.

(a) $K \neq J$: $^QR(J,K) = \ ^RQ(J,K) - \ ^RP(J+1,K)$

(b) $K \neq 0$: $^QR(J,K) = \ ^PQ(J,K) - \ ^PP(J+1,K)$

(c) $K \neq 0$: $^QR(J,K) = \ ^PR(J,K) - \ ^PQ(J+1,K)$

Fig. 5. Part of the energy level diagram demonstrating exemplarily close energy loops between ground and excited vibrational states. Three combination differences denoted as (a), (b) and (c) were used for calculating line pressure shifting of $^QR(J,K)$ ground state rotational transitions of CH_3D.

To the best of our knowledge, self-shifting has never been studied for the pure rotational lines of CH_3D as opposed to the lines of the excited vibrational states, e.g., for ν_5 [29], ν_6 [30], ν_3 [31], ν_2 [32] bands. Both positive and negative shifts were observed with values varying from line to line from -0.014 to 0.005 cm^{-1}/atm (-0.55 to 0.2 MHz/Torr). This data can be used for determining pressure shifting of the pure rotational lines $^QR(J,K)$ of the ground vibrational state. The calculation method follows from the energy diagram and selection rules (Fig. 5). Three combination differences denoted as a, b and c were applied to the experimental data of ν_5 [29] and ν_6 [30] bands to calculate the line pressure shifting of the $^QR(J,K)$ ground state rotational transitions of CH_3D. The results (see Table 2 and Fig. 6) were obtained for maximum $J_{max} = 5$ and exhibit good agreement both between the two calculated datasets and between the calculated and our experimental values, validating the results. It is worth noting that the available IR data allows calculating the line shifting for much higher J covering the whole range of experimental frequencies of ground state lines.

Pressure shifting, if not taken into account, causes systematic uncertainty when determining line center. The higher the pressure,
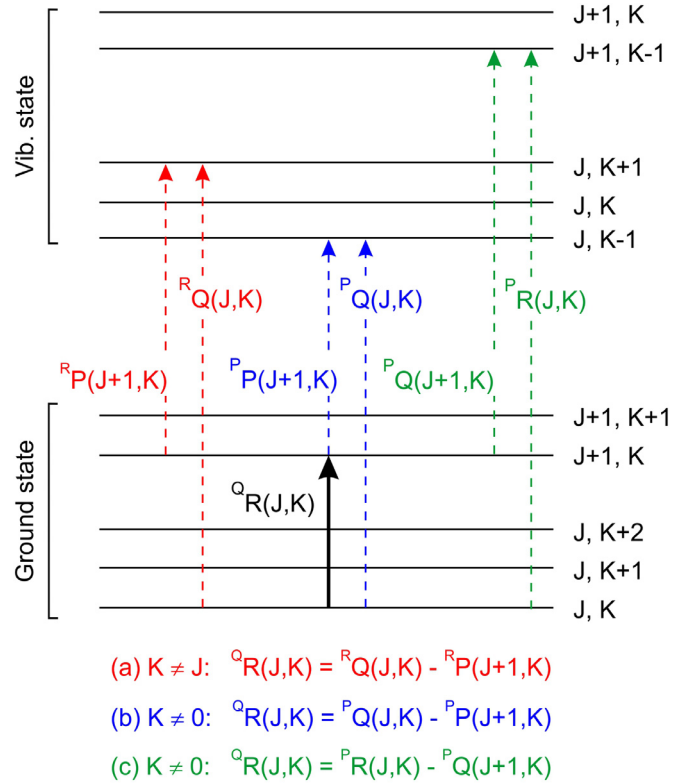
the larger the error is. Since line shifting was neglected in all previous experimental studies of the rotational spectra of CH_3D [11–15], the problem of the corresponding systematic error seems to be common. As an estimate, sample pressures were 0.1 Torr in [11], 0.05 Torr in [12], 0.28 Torr in [13] and 0.75 Torr in [15], which gave center shifting 8, 4, 24 and 64 kHz, respectively, with the use of our measured shift coefficient. We suppose that the use of the calculated shifts can slightly improve accuracy of determining line center. Otherwise, the corresponding uncertainties should be taken into account in the error budget by summing them with the statistical one, since both positive and negative shifts are equally probable. For the majority of the known THz/subTHz measurements, we estimate the value of the systematic error to be less or comparable with the statistical one.

Table 2

Self-shifting coefficients (in MHz/Torr) of $^Q R(J,K)$ ground state lines of CH_3D determined from the data of ν_5 [29] and ν_6 [30] bands. The combination differences used for calculation are marked by symbols a, b and c for each value (see details in Fig. 5).

| J	K	ν_6	ν_5
1	0	−0.278(21) [a]	0.174(9) [a]
	1	−0.007(13) [b]	0.088(9) [b]
			0.061(19) [c]
2	0	−0.131(27) [a]	0.110(7) [a]
	1	0.022(10) [a]	0.055(13) [a]
		0.079(10) [c]	0.017(8) [b]
			0.038(13) [c]
	2	0.114(11) [c]	0.083(8) [b]
3	0	−0.106(23) [a]	0.022(8) [a]
	1	0.009(7) [a]	0.025(7) [a]
		0.006(11) [b]	0.048(7) [b]
		0.041(10) [c]	0.062(13) [c]
	2	−0.095(22) [a]	0.041(16) [a]
		0.072(14) [c]	0.015(9) [b]
			−0.056(24) [c]
	3	0.063(17) [c]	0.066(19) [b]
4	0	−0.032(20) [a]	0.029(7) [a]
	1	0.019(8) [a]	0.025(5) [a]
		0.047(9) [b]	0.032(7) [b]
			0.005(14) [c]
	2	−0.010(8) [a]	0.039(8) [a]
		0.012(13) [b]	0.031(6) [b]
		0.071(14) [c]	−0.003(26) [c]
	3	0.029(8) [c]	−
	4	0.042(19) [b]	0.093(11) [b]
		−0.059(14) [c]	
5	0	−0.009(31) [a]	0.038(7) [a]
	1	0.056(8) [a]	0.005(6) [a]
		0.010(12) [b]	0.008(6) [b]
		0.035(10) [c]	0.118(26) [c]
	2	0.026(8) [a]	0.020(6) [a]
		0.009(8) [b]	0.005(6) [b]
		0.032(10) [c]	
	3	0.049(10) [a]	0.038(8) [a]
		−0.073(32) [b]	0.129(17) [b]
		0.248(22) [c]	
	4	0.058(9) [b]	−0.002(26) [a]
		−0.033(12) [c]	0.080(7) [b]
	5	0.084(9) [b]	0.144(13) [b]
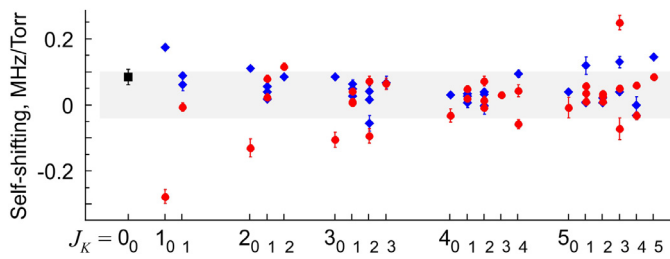
Fig. 6. Self-shifting coefficients of $^Q R(J,K)$ ground state lines of CH_3D calculated from IR data of ν_5 [29] (blue diamonds) and ν_6 [30] (red circles) bands. Our measured value for 1_0–0_0 line is shown by black square. Gray area demonstrates a standard deviation ±0.07 MHz/Torr of the points around its mean value 0.029 MHz/Torr. (For interpretation of the references to colour in this figure legend, the reader is referred to the web version of this article.)

4. Fitting the center positions and comparison with the previous works

As can be seen from Table 1, three frequencies of the ground state transitions measured by Womack et al. [12] and Pickett et al. [11] agree with our results within the combined experimental uncertainties. However, our values are more accurate. Weak lines of a series of Q-branch pure rotational transitions with J ranging from 1 to 11 and $\Delta K = +1$ belonging to the collisionally excited first

Table 3

Ground state effective Hamiltonian parameters of CH_3D (in MHz).

No	Parameter, tensorial nomenclature[*]	Value
1	$R2(0, 0A_1)$	130,021.9620(38)
2	$R2(2, 0A_1)$	8387.2084(23)
3	$R4(0, 0A_1)$	−2.368268(44)
4	$R4(2, 0A_1)$	$1.55723(16) \times 10^{-1}$
5	$R4(4, 0A_1)$	$7.06776(61) \times 10^{-2}$
6	$R4(4, 3A_1)$	$-2.35(28) \times 10^{-2}$
7	$R6(0, 0A_1)$	$1.1961(19) \times 10^{-4}$
8	$R6(2, 0A_1)$	$6.298(32) \times 10^{-6}$
9	$R6(4, 0A_1)$	$3.168(18) \times 10^{-6}$
10	$R6(6, 0A_1)$	$-1.445(49) \times 10^{-7}$
11	$R8(0, 0A_1)$	$-1.009(40) \times 10^{-8}$
12	$R8(2, 0A_1)$	$4.41(25) \times 10^{-10}$
13	$R8(6, 6A_1)$	$-2.08(21) \times 10^{-10}$

[*] See details in [35].

vibrational state ν_6 (1161 cm^{-1}) were also recorded. In the second vibrational state ν_3 (1306 cm^{-1}) of A_1 symmetry, three weak rotational transitions of the R branch, as well as one Q-branch rotational line within the third excited state ν_5 (1472 cm^{-1}) of E symmetry were observed.

To determine the parameters of the ground state, the THz transitions from Table 1 were included into the fit together with those measured previously [11–15] and listed in Table 1 in the work [15]. The pure rotational transitions in the first three excited states were also fitted by our effective polyad model constructed for the ground state and Triad interacting bands. The effective Hamiltonian was expressed in terms of irreducible tensor operators adapted to symmetric top C_{3V} molecules. This approach implemented in MIRS package [33,34] was previously applied for CH_3D [35-38], PH_3 [39], and recently for NF_3 [40,41]. The initial values of the effective Hamiltonian parameters were obtained by the contact transformation method [42,43] from the molecular potential energy surface [44] similarly to the procedure previously applied for CH_4 spectra analysis. The line intensities predicted [45,46] from the ab initio dipole moment surfaces [47,48] using the variational method [49] were employed for the line searching and transition assignments.

Rotational constants of the ground vibrational state corresponding to the K-dependence cannot be extracted from the pure rotational transitions due to $\Delta K = 0$ selection rule. Therefore, the GSCD method was applied to obtain pure rotational transitions from IR line positions of CH_3D analyzed previously in Triad [36,37], Nonad [37], and Enneadecad [38,50] regions of interacting bands. In Ref. [37] the assignments given in Refs. [51,52] were extended to all the nine bands of the Nonad. Finally, we fitted more than 11,900 rotational transitions including 77 known from THz measurements. Thirteen ground state parameters of the irreducible tensor operators were determined (Table 3) from the total number of 23 with the standard deviation of 0.216.

Eleven rotational transitions within the Triad vibrational states measured in this work (Table 1) were fitted with the IR transitions from [37] and experimental energy levels obtained by Ulenikov et al. [53]. For more than 3640 transitions and 680 levels, the achieved standard deviation of 0.516 corresponds to the accuracy of the majority of experimental data from [37]. The detailed statistical information on the fit of the parameters of the ground and ν_6, ν_3, and ν_5 excited states is presented in Table 4.

The determined ground state parameters reproduce in most cases (in 60 out of 77) the experimental THz transitions within their experimental uncertainty. Examples can be seen in Table 1 and Table 5 (a total list of the deviations is given in supplementary material I; supplementary material II contains rotational energy levels up to $J = 20$).

Table 4
Statistical information of the fit of the parameters of the ground and triad vibrational states of CH_3D.

Vibrational state	Number of data: THz/IR/levels	Sources*	J_{max}	σ
Ground	77 / 11,833 / 0	[11-15] TW / GSCD	20	0.216
ν_6	7 / 1575 / 290	TW / [37] / [53]	20	0.490
ν_3	3 / 641 / 121	TW / [37] / [53]	18	0.546
ν_5	1 / 1417 / 270	TW / [37] / [53]	18	0.530

* TW – results of this work; GSCD – transitions were determined by the ground state combination differences method (see details in the text); σ – standard deviation ($\sigma = \sqrt{(\sum((\nu_{obs} - \nu_{calc})/\delta\nu)^2)/N}$, N – number of the lines, $\delta\nu$ – uncertainty of the line center determination).

Table 5
Examples of the experimental transitions (in MHz) fitted in this work.

Exp.[e]	Exp.–Calc. (kHz)[f]		Assignment[h]
	This work	Ulenikov et al.[g]	J' K' Γ' –J'' K'' Γ''
465,235.553(13)[a]	−17	108	2 1 E – 1 1 E
465,250.725(10)[a]	8	111	2 0 A – 1 0 A
929,926.571(50)[b]	28	255	4 3 A – 3 3 A
1,162,125.166(100)[c]	−7	210	5 3 A – 4 3 A
1,394,135.500(70)[d]	21	171	6 3 A – 5 3 A
1,625,919.999(100)[c]	−156	9	7 3 A – 6 3 A
1,625,920.161(40)[d]	6	171	
1,857,442.241(70)[d]	195	63	8 3 A – 7 3 A
2,088,664.258(60)[d]	27	159	9 3 A – 8 3 A
2,319,550.084(90)[d]	−111	−645	10 3 A – 9 3 A
2,550,063.123(130)[d]	90	384	11 3 A – 10 3 A

[e] Experimental frequencies fitted in this work; a, b, c, and d correspond, respectively, to this work, to Ref. [13], Ref. [14], and Ref. [15].
[f] The root mean square deviations for all 77 transitions correspond to the values of 108 kHz and 230 kHz, respectively (see details in supplementary material I).
[g] Theoretical transitions were calculated on the basis of energy levels from Table 6 by Ulenikov et al. [54].
[h] Information on A_1–A_2 splitting is not presented in the experimental works used in the fitting.

Table 6
Comparisons of the fitting of pure rotational transitions of CH_3D.

Value	Drouin et al. [14]		Bray et al. [15]		This work	
	THz*	THz + GSCD**	THz*	THz + GSCD**	THz*	THz + GSCD**
N_{lines}	25	347	71	478	77	11,905
J_{max}	7	22	11	22	11	20
K_{max}	6	15	9	15	10	15
σ(THz)	0.293	0.422	0.742	0.314	0.742	0.751
σ(GSCD)		0.888		0.829		0.208
σ(Total)	0.293	0.779	0.742	0.891	0.742	0.216

* and ** parameters up to the sixth and eighth orders of the effective Hamiltonian were included, respectively, when fitting the transitions. The standard deviation (σ) has the same definition as in Table 4.

The THz transitions were fitted with the standard deviation close to that from the work by Bray et al. [15], when the parameters of the effective Hamiltonian up to the sixth order were used only (Table 6). Although Drouin et al. [14] fitted THz transitions with approximately 2.5 times smaller standard deviation (0.293 versus 0.742 in this work and Bray et al.), this was done with a smaller number of the experimental data ($J \leq 7$). All pure rotational transitions up to $J_{max} = 20$ were fitted with 0.216 standard deviation. This value is approximately four times less than that from the works by Drouin et al. [14] and Bray et al. [15] in which the transitions with $J_{max} = 22$ were also included in the fit. Since in this work more than 11,800 pure rotational transitions were obtained by the GSCD method, it was possible to determine the parameters of the effective Hamiltonian without fixing some of them to the results of the work [54] as it was done in Refs. [14,15].

The calculated rotational transitions within three excited states ν_6, ν_3, and ν_5 fall into experimental uncertainty in half of the cases. However, the number of the transitions is not so much to make the conclusion on the quality of the corresponding parameters, taking into account possible resonance interactions at higher J values.

Another problem is A_1/A_2 splitting that has not been resolved for pure rotational transitions of CH_3D yet. Accurate information about A_1/A_2 splittings can increase the accuracy of line list

positions and improve their modeling by the effective Hamiltonian. New accurate IR measurements with sub-Doppler resolution [55-58] can be very useful for analyzing the fine structures in molecular spectra. For CH_3D molecule, the A_1/A_2 splittings were mainly observed in the IR range for high-J transitions of the excited states (see, for example, Ref. [37,50,54]). However, in Ref. [58] the A_1/A_2 splittings were resolved for twenty three transitions of CH_3D corresponding to low-J levels of the ν_1 and ν_4 bands. These data will be useful for revising the A_1/A_2 splitting in all polyads of interacting states of CH_3D if new high-resolution IR spectra are available.

5. Conclusion

High sensitive measurements of pure rotational transitions of CH_3D by the radio-acoustic method are presented. Pressure broadening and shifting of the 1_0–0_0 ground state rotational line were accurately measured. Shift coefficients of the ground state rotational lines $^QR(J,K)$ with $J_{max} = 5$ were estimated using data for the lines of excited vibrational bands and confirmed our experimental results. The information on pressure shifting allowed estimating possible systematic errors of determining line positions. Among the 14 measured transitions, 3 correspond to the ground vibrational state. Other 11 lines were assigned to rotational transitions within the first three excited vibrational states: $\nu_6 = 1$,

$\nu_3 = 1$ and $\nu_5 = 1$. The measured frequencies of the ground state transitions agree with the previous experimental data but the results presented here are more accurate. These transitions together with the ones published previously were described in most cases within their experimental uncertainties using our effective Hamiltonian expressed in irreducible tensor operators. For determining the rotational parameters of the Hamiltonian, more than 11,800 ground state combination differences were also calculated and included in the fit. The obtained parameters will be used in our future works devoted to describing experimental intensities of pure rotational lines of CH_3D measured by various experimental groups including the ones measured in this work.

Declaration of Competing Interest

None.

CRediT authorship contribution statement

M.A. Koshelev: Conceptualization, Methodology, Investigation, Writing - original draft, Project administration. **I.N. Vilkov:** Investigation. **O. Egorov:** Formal analysis, Writing - original draft. **A.V. Nikitin:** Conceptualization, Methodology, Software. **M. Rey:** Software, Methodology.

Acknowledgements

Supplementary materials

Supplementary material associated with this article can be found, in the online version, at doi:10.1016/j.jqsrt.2019.106781.

References

[1] Linsky J, Draine B, Moos H, Jenkins EB, Wood BE, Oliveira C, Blair WP, Friedman SD, Gry C, Knauth D, Kruk JW, Lacour S, Lehner N, Redfield S, Shull JM, Sonneborn G, Williger GM. What is the total deuterium abundance in the local galactic disk? Astrophys J 2006;647:1106–24.

[2] Owen J, Jacque E. Astro- and cosmochemical consequences of accretion bursts – I. The D/H ratio of water. MNRAS 2015;446:3285–96.

[3] Encrenaz T. The planet Jupiter. Astron Astrophys Rev 1999;9:171–219.

[4] Penteado PF, Griffith CA, Greathouse TK, de Bergh C. Measurements of CH_3D and CH_4 in Titan from infrared spectroscopy. Astrophys J 2005;629:L53–6.

[5] Fletcher LN, Orton GS, Teanby NA, Irwin PGJ, Bjoraker GL. Methane and its isotopologues on Saturn from Cassini/CIRS observations. Icarus 2009;199:351–67.

[6] Irwin PGJ, de Bergh C, Courtin R, Bézard B, Teanby NA, Davis GR, Fletcher LN, Orton GS, Calcutt SB, Tice D, Hurley J. The application of new methane line absorption data to Gemini-N/NIFS and KPNO/FTS observations of Uranus' near-infrared spectrum. Icarus 2012;220:369–82.

[7] Irwin PGJ, Lellouch E, de Bergh C, Courtin R, Bézard B, Fletcher LN, Orton GS, Teanby NA, Calcutt SB, Tice D, Hurley J, Davis GR. Line-by-line analysis of Neptune's near-IR spectrum observed with Gemini/NIFS and VLT/CRIRES. Icarus 2014;227:37–48.

[8] Boudon V, Pirali O, Roy P, Brubach J-B, Manceron L, Vander Auwera J. The high-resolution far-infrared spectrum of methane at the SOLEIL synchrotron. J Quant Spectrosc Radiat Transf 2010;111:1117–29.

[9] Ozier I, Ho W, Birnbaum G. Pure rotational spectrum and electric dipole moment of CH_3D. J Chem Phys 1969;51:4873–80.

[10] Wofsy SC, Muenter JS, Klemperer W. Hyperfine structure and dipole moment of CH_3D. J Chem Phys 1970;53:4005–14.

[11] Pickett HM, Cohen EA, Phillips TG. Deuterated methane - Laboratory rotational spectrum and upper limits for its abundance in OMC-1. Astrophysical J 1980;236:L43–4.

[12] Womack M, Apponi AJ, Zirurys LM. Search for interstellar CH_3D: limits to the methane abundance in Orion-KL. Astrophys J 1996;46:897–901.

[13] Lattanzi V, Walters A, Pearson JC, Drouin BJ. THz spectrum of monodeuterated methane. J Quant Spectrosc Radiat Transf 2008;109:580–6.

[14] Drouin BJ, Shanshan Y, Pearson JC, Müller HSP. High resolution spectroscopy of $^{12}CH_3D$ and $^{13}CH_3D$. J Quant Spectrosc Radiat Transf 2009;110:2077–81.

[15] Bray C, Cuisset A, Hindle F, Bocquet R, Mouret G, Drouin B. CH_3D photomixing spectroscopy up to 2.5 THz: new set of rotational and dipole parameters, first THz self-broadening measurements. J Quant Spectrosc Radiat Transf 2017;189:198–205.

[16] Bray C, Cuisset A, Hindle F, Bocquet R, Mouret G, Drouin B. Corrigendum to "CH_3D photomixing spectroscopy up to 2.5 THz: new set of rotational and dipole parameters, first THz self-broadening measurements". J Quant Spectrosc Radiat Transf 2020;241:106758.

[17] Gordon IE, Rothman LS, Hill C, Kochanov RV, Tan Y, Bernath PF, Birk M, Campargue A, Boudon V, Chance KV, Drouin BJ, Flaud JM, Gamache RR, Hodges JT, Jacquemart D, Perevalov VI, Perrin A, Shine KP, Smith MAH, Tennyson J, Toon GC, Tran H, Tyuterev VG, Barbe A, Császár AG, Devi VM, Furtenbacher T, Harrison JJ, Hartmann J-M, Jolly A, Johnson TJ, Karman T, Kleiner I, Kyuberis AA, Loos J, Lyulin OM, Massie ST, Mikhailenko SN, Moazzen-Ahmadi N, Müller HSP, Naumenko OV, Nikitin AV, Polyansky OL, Rey M, Rotger M, Sharpe SW, Sung K, Starikova E, Tashkun SA, Vander Auwera J, Wagner G, Wilzewski J, Wcisło P, Yu S, Zak EJ. The HITRAN2016 Molecular Spectroscopic Database. J Quant Spectrosc Radiat Transf 2017;203:3–69.

[18] Jacquinet-Husson N, Armante R, Scott NA, Chédin A, Crépeau L, Boutammine C, Bouhdaoui A, Crevoisier C, Capelle V, Boonne C, Poulet-Crovisier N, Barbe A, Chris Benner D, Boudon V, Brown LR, Buldyreva J, Campargue A, Coudert LH, Devi VM, Down MJ, Drouin BJ, Fayt A, Fittschen C, Flaud J-M, Gamache RR, Harrison JJ, Hill C, Hodnebrog Ø, Hu S-M, Jacquemart D, Jolly A, Jiménez E, Lavrentieva NN, Liu A-W, Lodi L, Lyulin OM, Massie ST, Mikhailenko S, Müller HSP, Naumenko OV, Nikitin A, Nielsen CJ, Orphal J, Perevalov VI, Perrin A, Polovtseva E, Predoi-Cross A, Rotger M, Ruth AA, Yu SS, Sung K, Tashkun SA, Tennyson J, Tyuterev VIG, Vander Auwera J, Voronin BA, Makie A. The 2015 edition of the GEISA spectroscopic database. J Molec Spectrosc 2016;327:31–72.

[19] Pearson JC, Müller HSP, Pickett HM, Cohen EA, Drouin BJ. Introduction to submillimeter, millimeter and microwave spectral line catalog. J Quant Spectrosc Radiat Transf 2010;111:1614–16.

[20] Endres CP, Schlemmer S, Schilke P, Stutzki J, Müller HSP. The Cologne Database for Molecular Spectroscopy, CDMS, in the Virtual Atomic and Molecular Data Centre, VAMDC. J Molec Spectrosc 2016;327:95–104.

[21] Tyuterev VIG, Babikov YuL, Tashkun SA, Perevalov VI, Nikitin A, Champion JP, Hilico JC, Loete M, Pierre CL, Pierre G, Wenger Ch. T.D.S. spectroscopic databank for spherical tops. J Quant Spectrosc Radiat Transfer 1994;52:459–80.

[22] Ba YA, Wenger C, Surleau R, Boudon V, Rotger M, Daumont L, David Bonhommeau A, Tyuterev VIG, Dubernet M-L. MeCaSDa and ECaSDa: methane and ethene calculated spectroscopic databases for the virtual atomic and molecular data centre. J Quant Spectrosc Radiat Transf 2013;130:62–8.

[23] Tretyakov MYu, Koshelev MA, Makarov DS, Tonkov MV. Precise measurements of collision parameters of spectral lines with a spectrometer with radioacoustic detection of absorption in the millimeter and submillimeter ranges. Instrum Exp Tech 2008;51 78-8.

[24] Koshelev MA, Tsvetkov AI, Morozkin MV, Glyavin MYu, Tretyakov MYu. Molecular gas spectroscopy using radioacoustic detection and high-power coherent subteraherz radiation sources. J Molec Spectrosc 2017;331:9–16.

[25] Golubyatnikov GY, Koshelev MA, Tsvetkov AI, Fokin AP, Glyavin MY, Tretyakov MY. Terahertz high-sensitivity high-resolution molecular spectroscopy with a gyrotron. Submitted for JQSRT.

[26] Korolev AN, Zaitsev SA, Golenitskij II,. Zhary YV, Zakurdayev AD, Lopin MI, Meleshkevich PM, Gelvich EA, Negirev AA, Pobedonostsev AS, Poognin VI, Homich VB, Kargin AN. Traditional and novel vacuum electron devices, IEEE Trans Electron Devices 201;48:2929–37.

[27] Glyavin MYU, Chirkov AV, Denisov GG, Fokin AP, Kholoptsev VV, Kuftin AN, Luchinin AG, Golubyatnikov GYu, Malygin VI, Morozkin MV, Manuilov VN, Proyavin MD, Sedov AS, Sokolov EV, Tai EM, Tsvetkov AI, Zapevalov VE. Experimental tests of 263 GHz gyrotron for spectroscopy applications and diagnostic of various media. Rev Sci Instr 2015;86:054705.

[28] Fokin AP, Glyavin MYU, Golubyatnikov GYu, Lubyako LV, Morozkin MV, Movschevich BZ, Tsvetkov AI, Denisov GG. High-power sub-terahertz source with a record frequency stability at up to 1 Hz. Sci Rep 2018;8:4317.

[29] Devi VM, Benner DC, Smith MAH, Rinsland CP, Brown LR. Self- and N-broadening, pressure induced shift and line mixing in the ν_5 band of $^{12}CH_3D$ using a multispectrum fitting technique. J Quant Spectrosc Radiat Transf 2002;74:1–41.

[30] Devi VM, Benner CD, Smith MAH, Rinsland CP, Brown LR, Sams RL, Sharpe SW. Multispectrum analysis of self- and N_2-broadening coefficients, shifting and line mixing coefficients in the ν_6 band of $^{12}CH_3D$. J Quant Spectrosc Radiat Transf 2002;72:139–91.

[31] Devi VM, Benner CD, Smith MAH, Rinsland CP, Brown LR. Multispectrum analysis of self- and nitrogen-broadening, pressure shifting and line mixing in the ν_3 parallel band of $^{12}CH_3D$. J Quant Spectrosc Radiat Transf 2002;73:603–40.

[32] Predoi-Cross A, Hambrook K, Brawley-Tremblay M, Bouanich J-P, Devi VM, Benner CD, Brown LR. Measurements and theoretical calculations of self-broadening and self-shift coefficients in the ν_2 band of CH3D. J Mol Spectrosc 2005;234:53–74.

[33] Nikitin A, Champion JP, Tyuterev VIG. The MIRS computer package for modeling the rovibrational spectra of polyatomic molecules. J Quant Spectrosc Radiat Transf 2003;82:239–49.

[34] Nikitin AV, Rey M, Champion JP, Tyuterev VlG. Extension of the MIRS computer package for modeling of molecular spectra: from effective to full ab initio ro-vibrational Hamiltonians in irreducible tensor form. J Quant Spectrosc Radiat Transf 2012;113:1034–42.

[35] Nikitin AV, Champion JP, Tyuterev VlG, Brown LR. The high resolution infrared spectrum of CH_3D in the region 900–1700cm^{-1}. J Mol Spectrosc 1997;184:120–8.

[36] Nikitin A, Champion JP, Tyuterev VlG, Brown LR, Mellau G, Lock M. The infrared spectrum of CH_3D between 900 and 3200 cm^{-1}: extended assignment and modeling. J Mol Struct 2000;517-518:1–24.

[37] Nikitin A, Brown LR, Féjard L, Champion JP, Tyuterev VlG. Analysis of the CH_3D nonad from 2000 to 3300 cm^{-1}. J Mol Spectrosc 2002;216:225–51.

[38] Nikitin AV, Brown LR, Sung K, Rey M, Tyuterev VlG, Smith MAH, Mantz AW. Preliminary modeling of CH_3D from 4000 to 4550 cm^{-1}. J Quant Spectrosc Radiat Transf 2013;114:1–12.

[39] Nikitin AV, Ivanova YA, Rey M, Tashkun SA, Toon GC, Sung K, Tyuterev VlG. Analysis of PH_3 spectra in the octad range 2733–3660 cm^{-1}. J Quant Spectrosc Radiat Transf 2017;203:472–9.

[40] Rodina A, Egorov O, Nikitin A, Rey M, Serdyukov V, Sinitsa L, Tashkun S. Line list for NF_3 molecule in the 1750–1950 cm^{-1} region. J Quant Spectrosc Radiat Transf 2019;232:10–19.

[41] Egorov O, Nikitin A, Rey M, Rodina A, Tashkun S, Tyuterev V. Global modeling of NF_3 line positions and intensities from far to mid-infrared up to 2200 cm^{-1}. J Quant Spectrosc Radiat Transf 2019;239:106668.

[42] Tyuterev VlG, Perevalov VI. Generalized contact transformations of a Hamiltonian with a quasi-degenerate zero-order approximation. Application to accidental vibration- rotation resonances in molecules. Chem Phys Lett 1980;74:494–502.

[43] Tyuterev V, Tashkun S, Rey M, Kochanov R, Nikitin A, Delahaye T. Accurate spectroscopic models for methane polyads derived from a potential energy surface using high-order contact transformations. J Phys Chem A 2013;117:13779–805.

[44] Nikitin AV, Rey M, Tyuterev VG. Rotational and vibrational energy levels of methane calculated from a new potential energy surface. Chem Phys Lett 2011;501:179–86.

[45] Rey M, Nikitin AV, Tyuterev VlG. Accurate first-principles calculations for 12CH3D infrared spectra from isotopic and symmetry transformations. J Chem Phys 2014;141:044316.

[46] Rey M, Nikitin AV, Babikov Y, Tyuterev VlG. TheoReTS - An information system for theoretical spectra based on variational predictions from molecular potential energy and dipole moment surfaces. J Mol Spectrosc 2016;327:138–58.

[47] Nikitin AV, Rey M, Tyuterev VG. New dipole moment surfaces of methane. Chem Phys Lett 2013;565:5–11.

[48] Nikitin AV, Rey M, Tyuterev VG. Accurate line intensities of methane from first-principles calculations. J Quant Spectrosc Radiat Transfer 2017;200:90–9.

[49] Rey M, Nikitin AV, Tyuterev VG. First principles intensity calculations of the methane rovibrational spectra in the infrared up to 9300 cm^{-1}. Phys Chem Chem Phys 2013;15(25):10049–61.

[50] Nikitin AV, Champion J-P, Brown LR. Preliminary analysis of CH_3D from 3250 to 3700cm^{-1}. J Mol Spectrosc 2006;240:14–25.

[51] Chackerian C Jr, Guelachvili G. Ground-state rotational constants of $^{12}CH_3D$. J Mol Spectrosc 1980;84:447–56.

[52] Chackerian C Jr, ES Bus, Olson WB, Guelachvili G. Determination of A_0 for CH_3D from perturbation-allowed transitions. J Mol Spectrosc 1986;117:355–60.

[53] Ulenikov ON, Onopenko GA, Tyabaeva NE, Schroderus J, Alanko S. Study on the rovibrational interactions and a_1/a_2 splittings in the $\nu_3/\nu_5/\nu_6$ triad of CH_3D. J Mol Spectrosc 2000;200:1–15.

[54] Ulenikov ON, Onopenko GA, Tyabaeva NE, Schroderus J, Alanko S. On the rotational analysis of the ground vibrational state of CH_3D molecule. J Mol Spectrosc 1999;193:249–59.

[55] Abe M, Iwakuni K, Okubo S, Sasada H. Accurate transition frequency list of the ν_3 band of methane from sub-Doppler resolution comb-referenced spectroscopy. J Opt Soc Am B 2013;30:1027–35.

[56] Iwakuni K, Okubo S, Sasada H. A novel frequency control scheme for comb-referenced sensitive difference-frequency-generation spectroscopy. Opt Express 2013;21:14832–40.

[57] Abe M, Iwakuni K, Okubo S, Sasada H. Design of cavity-enhanced absorption cell for reducing transit-time broadening. Opt Lett 2014;39:5277–80.

[58] Abe M, Sera H, Sasada H. A_1–A_2 splitting of CH_3D. J Mol Spectrosc 2015;312:90–6.